Spectral light transmission measure of metal screens for glass façades and assessment of their shading potential

Andrea G. Mainini[a,]*, Tiziana Poli[a], Michele Zinzi[b], Alberto Speroni[a]

[a]Politecnico di Milano - Architecture, Built environment and Construction engineering Dept., P.zza Leonardo da Vinci 32, Milano 20133, Italy [b]ENEA – UTEE ERT, Via Anguillarese 301, Roma 00123, Italy

* Corresponding author. Tel.: +39 0223996015; fax: +39 0223996020.
E-mail address: andreagiovanni.mainini@polimi.it , mainini.andrea@gmail.com

1. **Introduction**

The transparency of metal mesh grids and perforated metal sheets is normally evaluated by the openness factor, which is the ratio between transparent and opaque surfaces. In the first case the ratio depends on the spacing and thread dimension of metal wires, and in the second case depends on the spacing and average dimension of the holes. The shading performance is related to the incidence angle of the solar radiation on the screen surface, affecting its light and solar transmittance.

To assess the effetiveness of metal screens as shading device the radiative properties (spectral reflectance of metal surfaces and coating) , wire shape and texture (for metal mesh grids) or holes shape and distribution (for perforated and stamped metal sheets) need to be properly defined.

The study here presented mainly concerns three categories of metal screens: perforated metal sheets, stamped metal sheets and metal mesh grids. The results are also presented in comparison with the performances of a PTFE fabric metal coated sunscreen with a metal coated traditional fabric shading system.

2. Samples description

The selected samples present a similar openness factor , about 40%, but different geometry in order to evaluate the incidence of the geometry of the shadings on the visible and solar angular transmittance performances.

The samples tested are showed in Fig.1 and are:

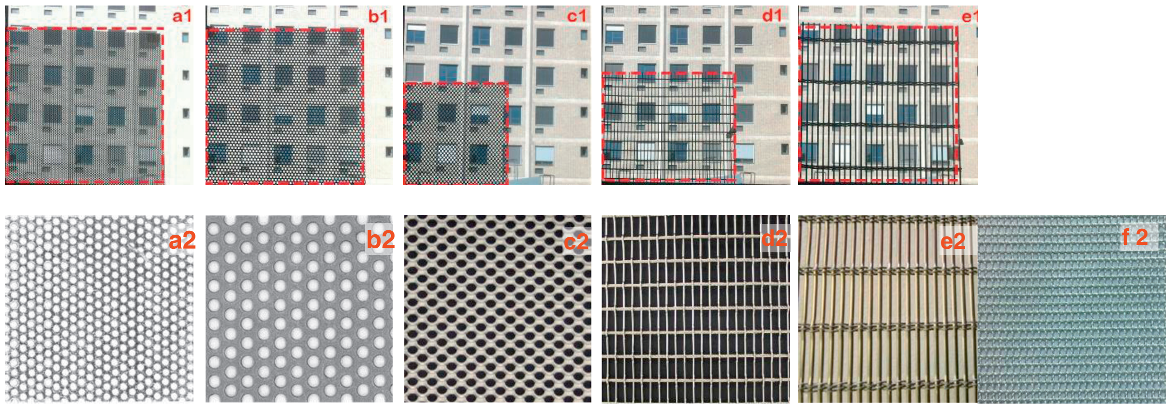

Fig. 1 – Samples: a1) Test application of sample R2T3, b1) Test application of sample R4T6, c1) Test application of sample 06003, d1) Test application of sample 00003, e1) Test application of sample A401, a2) Sample R2T3, b2) Sample R4T6, c2) Sample 06003, d2) Sample 00003, e2) Sample A401, f2) Sample 11016.

Both selected perforated metal sheets have circular holes, arranged in staggered rows at 60°, with the same openness factor (40%), but with different diameters and distances between the holes. The first sample (R2T3) has holes with a diameter of 2 mm and a pitch of 3 mm while the second sample (R4T6) has holes with a diameter of 4 mm and a pitch of 6 mm. The surface of both the sheets is planar and all the holes have the same thickness. The choice of the samples depends on the possibility to evaluate the relation between the diameter of the holes and the thickness of the sheet and how this relation affects the inter-reflections, and then, for increasing angles of incidence, the comparison for transmittance values decrement between the two sheets.

As shown in Fig.1 the selected stamped metal sheet (06003 table 1) has holes arranged in staggered rows at 60°, with an openness factor similar to the one of the perforated metal sheets (38%). The differences between the perforated metal sheets refers to the geometry of the holes and are related to the non-planar surface of the sheet, due to the particular 3D texture of the sample.

Table 1. Perforated metal sheets and stamped metal sheets samples features.

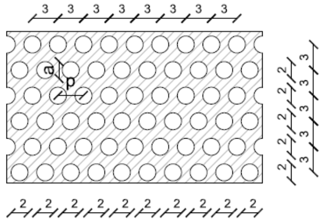
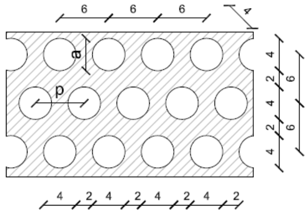
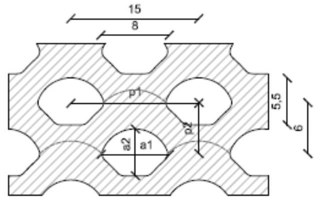

R2T3		R4T6		06003	
a [mm]	2	a [mm]	4	a1[mm]	8
p [mm]	3	p [mm]	6	a2[mm]	5,5
Openness factor [%]	40	Openness factor [%]	40	p1 [mm]	15
Max. width [mm]	1300	Max. width [mm]	1500	p2 [mm]	6
Thickness [mm]	1	Thickness [mm]	1	Openness factor [%]	38
Material	Steel	Material	Steel	Thickness [mm]	1,5
Property	Round holes	Property	Round holes	Material	Steel

Table 2. Metal mesh grid and PTFE fabric features.

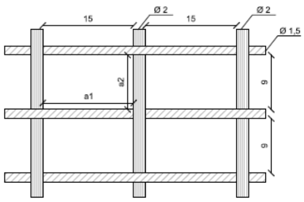
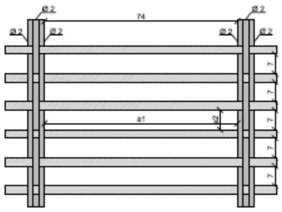
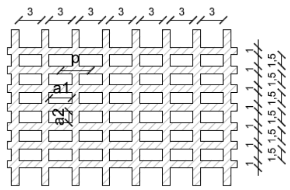

00006		A401		11016	
a1[mm]	15	a1[mm]	74	a1[mm]	3
a2[mm]	9	a2[mm]	7	a2[mm]	1,5
Openness factor [%]	44	Openness factor [%]	46	p [mm]	4
Max. width [mm]	2000	Max. width [mm]	3000	Openness factor [%]	40
Thickness [mm]	4,5	Thickness [mm]	6,5	Thickness [mm]	0,5
Material	Stainless steel	Material	Stainless steel	Material	PTFE
Property	Wire Ø 1,5; 2	Property	Wire Ø 3; 2	Property	Square holes

The metal mesh grids selected are two, both made by stainless steel with similar openness factor. The first sample (00006) has an openness factor of 44% made up by longitudinal cord with a diameter of 2 mm and a pitch of 15 mm, and transversal cord with a diameter of 1,5 mm and a pitch of 9 mm; the total thickness is 4,5 mm. The second sample (A401) is a wire cloth with openness factor of 46% made up by longitudinal cord with a diameter of 2 mm and a pitch of 74 mm, and transversal cord with a diameter of 3 mm and a pitch of 7 mm; the total thickness is 6,5 mm. Furthermoreit has been selected an additional sample of PTFE (11016) characterized by a square mesh (3x1, 5 mm) with a 40% percentage of open area, as a comparison.

3. Experimental

3.1. Experimental set-up description

To evaluate solar and light properties of the chosen samples a standard spectrophotomer cannot be used, because the samples are characterized by a large dimension texture and the incident radiation beam area must be large enough to irradiate a significant portion of the sample itself. Large integrating sphere are needed to perform accurate measurements on such samples [1].

The experimental set-up is here described:

- A 300 Watt tungsten free halogen lamp with a light beam diameter that can be modulated through a diaphragm according to the measurement requirements;
- The light source is mounted on a holder, which can rotate arm in order to vary the beam angle of incidence;
- An integrating sphere with a 75 centimeters diameter. The external shell of the sphere is made of aluminium, while the internal surface coated with a non-selective material with a reflectivity greater than 90% between (300-2500 nanometers). The sphere is equipped with several auxiliary ports and can be adjusted in order to perform transmittance, reflectance and absorbance measurements;
- Detection system consisting of three array spectrometers and the three following detectors: NMOS for the 250-1000nm range (dispersion 1.4 nm/pixel); InGaAs for the 900-1700nm range (dispersion 3.125 nm/pixel); ExtInGaAs for the 1600-2500nm range (dispersion 3.52 nm/pixel).The first two detector was effectively used in this campaign, since only the sample characteristics in the UV, Visible and part of the NIR range were investigated.

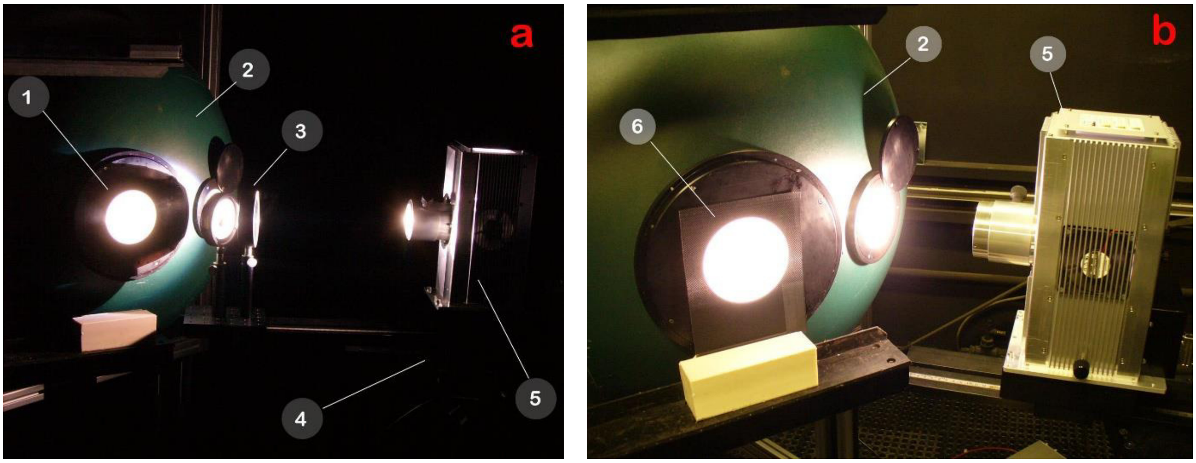

Fig. 2 – (a) Optical bench; (b) Substitution Error set-up: 1) Sample port, 2) integrating sphere, 3) diaphragm, 4) light source holder, 5) Light source

The procedures are following described:

- The sample port is 25 cm in diameter and the incident beam diameter is optimized for the measurement of all the samples;
- The transmittance is measured as the ratio of the energy transmitted by the specimen mounted on the sample port on the energy directly entering the sphere. The measurement is corrected with the auxiliary port correction method [2],[3];
- The measurements are performed at the following incidence angles: 0°, 30°, 45°, 60°;

- Measurements were performed between 300 and 1700nm, covering the whole visible range and the 95.6% of the whole solar range. The solar quantities were calculated from the spectral data using the reference solar spectrum defined in [4].

3.2. Angular integrated light and energy transmittance measure results

Angular integrated light transmittance (τ_v) and angular integrated solar transmittance (τ_e for only the 95.6% of the solar spectrum) values were calculated for all of the samples. Comparative results show that for each sample τ_v is similar to τ_e because of the particular sample used. To reduce the number of graphic signs τ is representative for both the properties. The integrated values for τ_v and τ_e are reported in the tables under or on the side of the graphs.

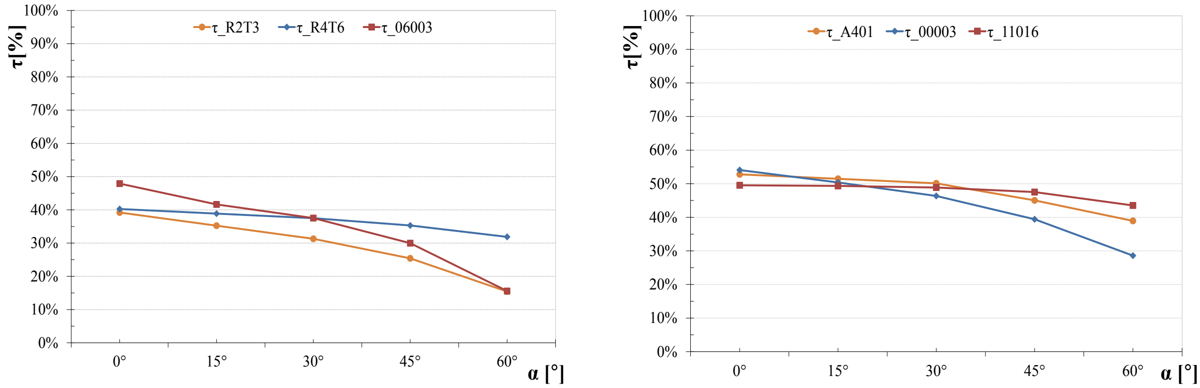

Fig. 3 - (a) Comparison of transmittance values between samples R2T3, R4T6 and 06003and (b) Table 2 - Comparison between samples A401, 00003, 11016.

Table 3. (a) Comparison of transmittance values between samples R2T3, R4T6 and 06003and (b) - Comparison between samples A401, 00003, 11016.

Sample	**0°**	**15°**	**30°**	**45°**	**60°**
τ_e_R2T3	39,2%	35,3%	31,4%	25,5%	15,6%
τ_v_R2T3	39,2%	35,2%	31,2%	25,3%	15,3%
τ_e_R4T6	40,2%	38,8%	37,5%	35,3%	31,9%
τ_v_R4T6	40,3%	38,9%	37,5%	35,4%	31,9%
τ_e_06003	48,1%	41,8%	37,7%	30,1%	16,0%
τ_v_06003	47,7%	41,5%	37,4%	29,8%	15,2%

Sample	**0°**	**15°**	**30°**	**45°**	**60°**
τ_e_A401	53,0%	51,7%	50,3%	45,2%	39,0%
τ_v_A401	52,6%	51,3%	50,0%	44,9%	38,8%
τ_e_00003	54,3%	50,7%	46,7%	39,8%	29,1%
τ_v_00003	53,9%	50,0%	46,0%	39,0%	28,1%
τ_e_11016	49,7%	49,5%	49,0%	47,7%	43,7%
τ_v_11016	49,4%	49,2%	48,8%	47,4%	43,4%

The comparison between the two perforated metal sheets, with the same openness factor, and the stamped metal sheet (Fig.3a and Table 3a) show that:

- the sample R2T3 has solar and light values that greatly decrease with an increasing of the angle of incidence, passing from 39% to 15%. The sample R4T6 has a similar behavior but with a smaller transmittance coefficient decrease, in fact it varies from an initial transmission coefficient of 40% to 32% at 60 °. This difference is due to higher inter-reflections in the denser mesh (R2T3) so the different results between the two samples are a consequence of their geometry. Both samples have the same thickness, but the ratio between average hole diameter and thickness is an important parameter to define the angular optical performance of the perforated metal sheet;

- The stamped metal sheet has the greatest decreasing of the transmittance coefficient for an increasing of the angle of incidence thanks to its 3d geometry correctly orientated (see table 3 description). The 0° transmittance is also greater than the other samples, despite of the reduced openness factor (38%). This particular behavior depends on the non-planar faces of the samples as you can see in Fig 1

The comparison between the two metal mesh grid with the PTFE fabric show that, as for perforated metal sheet, the greatest contribute in reducing the transmittance values depends, for increasing incident angles, by the ratio between the spacing and thread of the wire. If the average thickness of the sample is comparable to the holes dimension there is an efficient reduction in angular transmittance values.

For both metal mesh grid and stamped metal sheets the angular measure transmittance values not only depends on the openness factor, but also on their orientation, because of their geometry. The change in orientation of the samples on the sample port (a rotation on the port plane) determines a variation on measured transmittance values for the same incidence angles of the light beam. This is not significant for the others, because of their symmetric geometry between the two axis (x,y) of the sample.

The sample that has the transmittance values more influenced by the orientation is the stamped metal sheet. The results are presented in Fig. 4 and Table 4, for 5 incident angles of the light beam (0° to 60°) and for 4 different orientation of the sample, from 0° to 270° with a clockwise rotation step of 90°. For metal mesh grid angular transmittance values change just for two orientation step (0°-90°) and the results are not here reported.

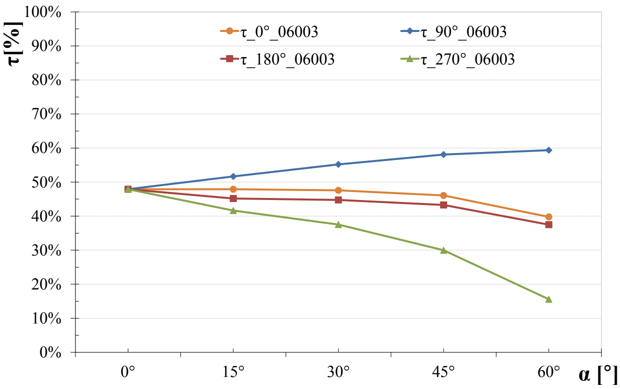

Fig. 4 - Sample 06003: angular transmittance values for different orientation of the sample on the sample port.

Table 4. Sample 06003: angular transmittance values for different orientation of the sample on the sample port.

Sample	**0°**	**15°**	**30°**	**45°**	**60°**
τe_0°_06003	48,1%	48,1%	47,8%	46,3%	40,2%
τv_0°_06003	47,7%	47,7%	47,4%	45,9%	39,3%
τe_90°_06003	48,1%	51,8%	55,4%	58,3%	60,0%
τv_90°_06003	47,7%	51,5%	55,0%	57,8%	58,8%
τe_180°_06003	48,1%	45,3%	44,9%	43,4%	37,7%
τv_180°_06003	47,7%	45,1%	44,6%	43,2%	37,3%
τe_270°_06003	48,1%	41,8%	37,7%	30,1%	16,0%
τv_270°_06003	47,7%	41,5%	37,4%	29,8%	15,2%

4. Simulation

Optimal sun shading systems need to provide thermal comfort preventing unwanted solar gains in summer and allowing high solar gains in winter. In reality, the effectiveness of these systems need to be properly simulated (and tested) in order to obtain adequate design parameters [5,6].

Because of their flexibility, geometry and design, metal meshes could be considered as a textile or generally similar to a woven surface. Those systems have recently been applied as a second skin on opaque and transparent building façade and they have been mainly used as permanent sun shading systems.

Three simple geometry of metal mesh grid made by stainless steel and characterized by the periodicity of the weave and the thread structure, where simulated using LBNL Window 6.2 woven shade BSDF file generator and the results were processed with the aid of a post processing LBNL macro included in this software release [7].

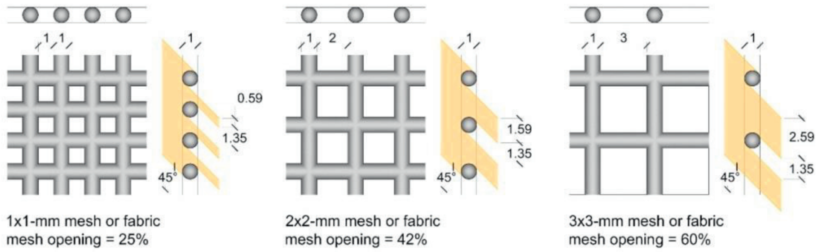

Fig. 5 - Different geometries of fabric and metal meshes sorted by mesh opening (dimensions in mm).

The geometries of the meshes are simple with a square pattern with round, 1-mm-diameter wires (or threads) for both weave and warp and 1x1-mm, 2x2-mm or 3x3-mm mesh opening. With this geometrical morphology, the resulting meshed surfaces have opening factors of 25%, 42% and 60%, as shown Fig.5. The integrated value of solar reflectance for metal wire of the model is set to 0.7.

Each combination of type and geometry has been studied through software simulation for each orientation (East, South, West, South-East, South-West) and for three Italian different latitudes depending on the location:

- Milan (lat. 45.48°; long. 9.18°);
- Rome (lat. 41.91°; long. 12.48°);
- Palermo (lat. 38.11°; long. 13.34°).

	Jan	Feb	Mar	Apr	May	Jun	Jul	Aug	Sep	Oct	Nov	Dec
12am	0.000	0.000	0.000	0.000	0.000	0.000	0.000	0.000	0.000	0.000	0.000	0.000
1am	0.000	0.000	0.000	0.000	0.000	0.000	0.000	0.000	0.000	0.000	0.000	0.000
2am	0.000	0.000	0.000	0.000	0.000	0.000	0.000	0.000	0.000	0.000	0.000	0.000
3am	0.000	0.000	0.000	0.000	0.000	0.000	0.000	0.000	0.000	0.000	0.000	0.000
4am	0.000	0.000	0.000	0.000	0.000	0.000	0.000	0.000	0.000	0.000	0.000	0.000
5am	0.000	0.000	0.000	0.000	0.000	0.000	0.000	0.000	0.000	0.000	0.000	0.000
6am	0.000	0.000	0.092	0.000	0.000	0.000	0.000	0.000	0.092	0.000	0.000	0.000
7am	0.000	0.146	0.090	0.089	0.000	0.000	0.000	0.089	0.090	0.146	0.000	0.000
8am	0.340	0.267	0.174	0.087	0.087	0.087	0.087	0.087	0.174	0.267	0.340	0.355
9am	0.381	0.360	0.284	0.170	0.085	0.085	0.085	0.170	0.284	0.360	0.381	0.388
10am	0.409	0.387	0.359	0.252	0.159	0.121	0.159	0.252	0.359	0.387	0.409	0.414
11am	0.422	0.407	0.376	0.309	0.211	0.171	0.211	0.309	0.376	0.407	0.422	0.428
12pm	0.428	0.412	0.381	0.327	0.230	0.190	0.230	0.327	0.381	0.412	0.428	0.434
1pm	0.422	0.407	0.376	0.309	0.211	0.171	0.211	0.309	0.376	0.407	0.422	0.428
2pm	0.409	0.387	0.359	0.252	0.159	0.121	0.159	0.252	0.359	0.387	0.409	0.414
3pm	0.381	0.360	0.284	0.170	0.085	0.085	0.085	0.170	0.284	0.360	0.381	0.388
4pm	0.340	0.267	0.174	0.087	0.087	0.087	0.087	0.087	0.174	0.267	0.340	0.355
5pm	0.000	0.146	0.090	0.089	0.000	0.000	0.000	0.089	0.090	0.146	0.000	0.000
6pm	0.000	0.000	0.092	0.000	0.000	0.000	0.000	0.000	0.092	0.000	0.000	0.000
7pm	0.000	0.000	0.000	0.000	0.000	0.000	0.000	0.000	0.000	0.000	0.000	0.000
8pm	0.000	0.000	0.000	0.000	0.000	0.000	0.000	0.000	0.000	0.000	0.000	0.000
9pm	0.000	0.000	0.000	0.000	0.000	0.000	0.000	0.000	0.000	0.000	0.000	0.000
10pm	0.000	0.000	0.000	0.000	0.000	0.000	0.000	0.000	0.000	0.000	0.000	0.000
11pm	0.000	0.000	0.000	0.000	0.000	0.000	0.000	0.000	0.000	0.000	0.000	0.000

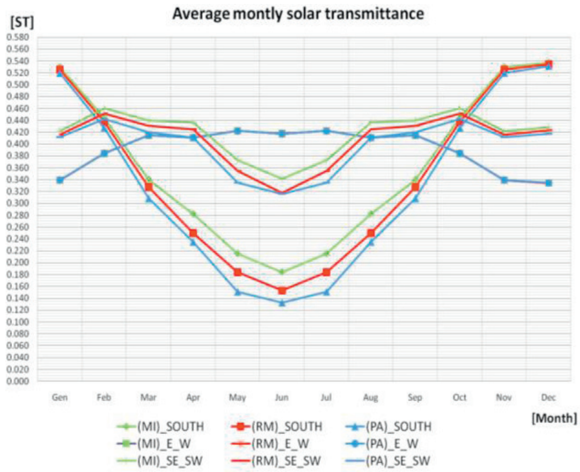

Fig. 6 – (a) Solar transmittance values during the year (Milan, South, Type 1, 3x3-mm mesh).(b) Comparison between solar transmittance values during the year (Milan, Rome and Palermo over 5 orientations South, East, West, South-East, South West, Type 1, 3x3-mm mesh)

The obtained output is the solar transmittance value of a generic mesh component depending on the mesh openness factor, orientation, latitude, day and hour, which have an influence on the solar incidence angle on surfaces and on the interreflections between the metal mesh wires. Parametric simulations allow to obtain the average hourly monthly solar transmittance for every data set.

In Fig. 6a and b, as part of simulation results, the average monthly solar transmittance values are shown. The calculation focus on a function that calculates bi-directional properties (for transmittance and reflectance), which are defined for each combination of incident and outgoing direction, and that builds BTDF and BRDF matrices for all incident and outgoing directions as result.

In accordance with the simulation results of bidirectional transmittance of metal wire meshes, some energy balance evaluations of a case study, through a TRNSYS 16 [8,9] dynamic model, are used to evaluate the effectiveness of those systems. The case study consists in a standard office space in a mid-size office building with a curtain wall façade and metal wire meshes parallel to the façade, used as a sun-shading system (Fig, 7 a,b, c). The office is located in the middle of the building and all the thermal losses are due to the curtain wall facing outdoors and to ventilation (without energy recovery system).

Here are some of the simulation parameters considered:

- Gross/Net internal surface: 19.20 / 17.5 m^2;
- Gross/Net internal volume: 64.26 / 52.50 m^2;
- Internal gains due to people and appliances 18 W/m^2;
- Hourly air exchanges: 0.95 vol/h;
- Boundary surfaces: Plaster board insulated walls and ceilings, floating wood floor

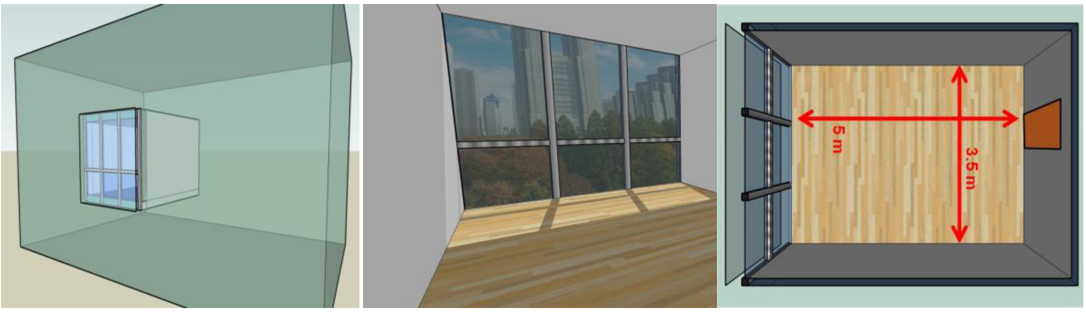

Fig. 7 – (a,b,c) The reference standard office considered in the simulation.

Two different approaches for transparent surfaces shading for the building are here compared, both considering the use of static device systems to control solar gains.

Evaluations of summer cooling and winter heating loads are done for the standard office (Net Energy) to compare the effectiveness of both solutions in reducing solar gains and in decreasing energy consumption in summer, without compromising the maximum availability of solar gains during winter.

The results in Fig. 7 refer to a two standard office with two curtain walls with different type of double pane insulated glass: one equipped with a colored bronze glass with a very low g-value and the other one with a clear low-e double pane insulated glass and a metal mesh grid 3x3 mm shading system. Here are the properties of the window panes used:

Table 5. Glass panes properties.

Glass type	U factor [W/m^2 K]	Dimension [mm]	g [-]
Low_e_clear glass	1.416	4-12-4	0.568
Low_g glass	1.452	4-12-4	0.300

The results are presented in Fig.8 and two situations are compared for two different orientation of the glass façade. Only the net energy demand , expressed in kWh/m^3 month, was evaluated.

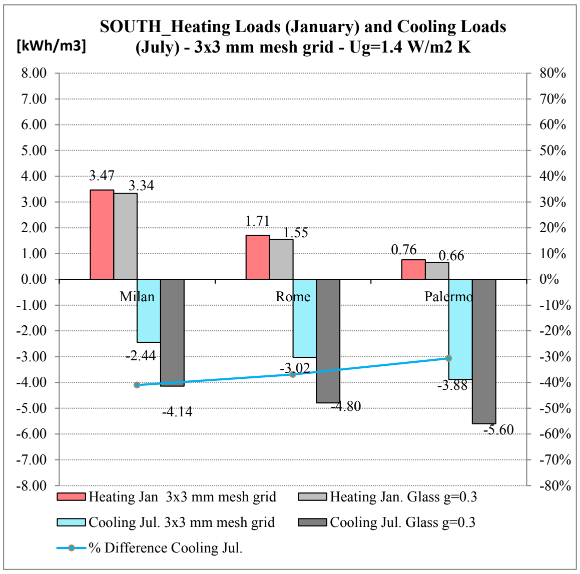

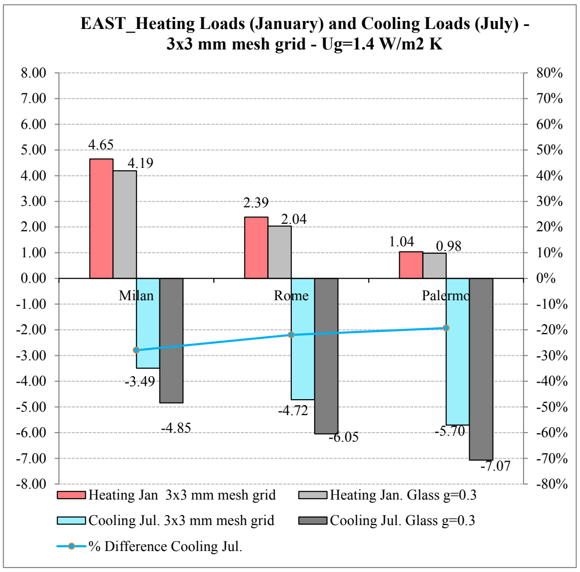

Fig. 8 –Comparison between the two solar control strategies for the reference standard office considered. Net energy demand comparison for 3 Italian Latitudes depending on location (Milan, Rome, Palermo) and orientation of the curtain wall. (a) South (b) East

5. Conclusions

The openness factor of perforated and stamped metal sheet, as the openness factor of metal mesh grid and metal coated fabric is not an adequate parameter to define their performances as solar shading systems.

The results in angular light and solar transmittance measurement are strongly affected by the geometry and the ratio between the openness standard dimension and the thickness of the panel. an additional evaluation, in accordance with the orientation and the predicted sun position, should be done to determine the position (rotation on the façade plane) of the shading system, to maximize the direct light and solar transmittance reduction, also considering daylighting requests[10].

The solar transmittance for a generic metal mesh grid does not have a wide variability of results for East or West Orientation. Concerning South orientation, the solar transmittance substantially varies and reaches its minimum during summer months and its maximum during winter months, as a requested performance for an optimal shading device. Latitude influences results for South orientation too. Southern locations have smaller solar transmittance than northern ones.

For the same weather conditions, the test case with a low-g glass have higher cooling loads than the ones with the clear glass and the shading system. The difference in cooling loads can reach up to the 40%.

In addition perceived mean radiant temperature in the first case is 3-4°C higher than in the second one

Parametric studies on the variation of the solar gains were also conducted to define their dependency on the solar reflectance of the metal wire coating. The results show that during summer months the incidence of the solar reflectance is stronger than in the winter ones.

Acknowledgements

The authors thank Dr. Emiliano Carnielo, Università degli Studi Roma Tre and Lorenzo Vercesi for the cooperation and the precious help for further and future developments.

The authors also thank Matteo Birocchi, Politecnico di Milano, for the cooperation in the early development stages of this paper.

We also gratefully thank all the manufacturers that provided the samples.

References

[1] Mainini AG, Poli T, Zinz i M, Cangiano S. Spectral Light Transmission Measure and radiance Model Validation of an innovative transparent concrete Panel for Facades. Energy Procedia 2012; 30:1184-1194.

[2] CIE 130 Practical methods for the measurement of reflectance and transmittance. Commission Internationale de l' éclarage. Vienna; 1998.

[3] Maccari A, Montecchi M, Treppo F, Zinzi M. Applied optics 1998;37:5156-5161.

[4] ISO 9050 Glass in building Determination of light transmittance, solar direct transmittance, total solar energy transmittance, ultraviolet transmittance and related glazing factors; 2003.

[5] Al-Shareef FM, Oldham DJ, Carter DJ. A computer model for predicting the daylight performance of complex parallel shading systems. Building and environment 2001; 36:605-618.

[6] Kim G, Lim HS, Lim TS, Schaefer L, Kim TJ, Comparative advantage of an exterior shading device in thermal performance for residential buildings. Energy and buildings 2012;46:105-111

[7] Mitchell R et al. Window 5.0 User Manual. California: LBNL; 2001.

[8] Campora M, Keilholz W, Sette P et al. Using Simulation Studio. In TRNSYS 16 Transient System Simulation program user manual. CSTB; 2007. p. 1-126

[9] SEL, TRNSSOLAR, CSTB, Tess. Multizone Building modeling with Type56 and TRNBuild. In TRNSYS 16 a Transient System Simulation program user manual. Madison: University of Wisconsin-Madison; 2007. p. 1-213

[10]Sherif A, Sabry H, Rakha T. External perforated Solar Screens for daylighting in residential desert buildings: Identification of minimum perforation percentages. Solar Energy 2012;86: 1929-1940.